Mitochondria-Localized Fluorescent BODIPY-Platinum Conjugate

Tingting Sun,[†,‡] Xingang Guan,[†,§] Min Zheng,*[,‖] Xiabin Jing,[†] and Zhigang Xie*[,†]

[†]State Key Laboratory of Polymer Physics and Chemistry, Changchun Institute of Applied Chemistry, Chinese Academy of Sciences, Changchun 130022, P. R. China

[‡]The University of Chinese Academy of Sciences, Beijing 100049, P. R. China

[§]Life Science Research Center, Beihua University, Jilin 132013, P. R. China

[‖]State Key Laboratory of Luminescence and Applications, Changchun Institute of Optics, Fine Mechanics, and Physics, Chinese Academy of Sciences, 3888 East Nanhu Road, Changchun, Jilin 130033, P. R. China

S *Supporting Information*

ABSTRACT: A convenient synthesis of a BODIPY (1,3,5,7-tetramethyl-8-(4-pyridyl)-4,4′-difluoroboradiazaindacene) labeled platinum compound (BODIPY-Pt) was developed by direct conjugation of cisplatin with the pyridine group of BODIPY. The membrane permeability and selective uptake of BODIPY-Pt in the mitochondria was studied using confocal laser scanning microscopy (CLSM). The fluorescent BODIPY-Pt conjugate showed high cellular proliferation inhibition against human cervical carcinoma (HeLa) and human breast cancer (MCF-7) cells, with half maximal inhibitory concentrations (IC$_{50}$) of 27.37 and 12.14 μM, respectively. This work highlights the potential of using BODIPY labeled Pt compounds to realize the visualization of Pt distribution in living cells.
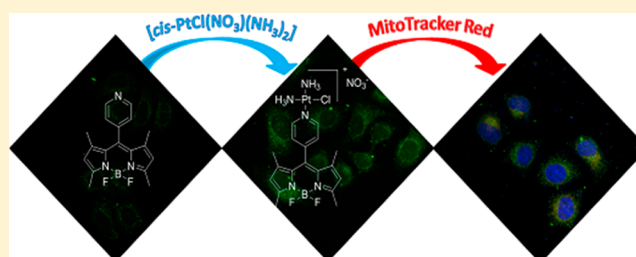
KEYWORDS: BODIPY, cisplatin, mitochondria, imaging

Platinum compounds have emerged as powerful anticancer drugs for decades against a variety of solid malignancies, like bladder, ovarian, head and neck, testicular, and lung cancers.[1,2] Pt drugs, cisplatin and carboplatin, alone or in combination with other drugs, are used to treat 40−80% of cancer patients.[3,4] Nonetheless, side effects combined with limited pharmacokinetic properties remain significant drawbacks.[5−7] Therefore, there is a growing demand for overcoming toxicity and efficacy issues. One approach is design and development of new Pt complexes that modulate the molecular process and pathways associated with tumor suppression.[8,9]

Mitochondria represent interesting targets for drug development. A wide range of pathologies including cardiovascular disorders,[10] diabetes,[11] neurodegenerative diseases,[12,13] and cancers are related with mitochondrial dysfunction.[14] Some of the processes involving nucleic acids in the nuclei can also occur in the mitochondria of human cells, and mitochondrial DNA (mtDNA) plays significant roles in cell death and metastatic competence. Kelley et al. have engineered the first mitochondria targeted version of doxorubicin (Dox), which maintains the ability to inhibit TopoII and damage mtDNA selectively.[15] Chemoresistance of cisplatin therapy may result from several mechanisms,[16−18] which include decreased uptake and accelerated DNA repair by nucleotide excision repair (NER) machinery. The enhanced mtDNA mutation and lack of NER machinery in the mitochondria of aggressive cancer cells offers a great postulate in directing cisplatin into the mitochondrial matrix to provide an effective therapeutic method.[19] However, rare studies have examined cisplatin activity on mtDNA of cancer cells.[20] Therefore, it is highly desired to develop a mitochondria-localized cisplatin formulation to gain further insight into the mechanisms of action.

It is impossible to image Pt distribution and metabolism in living cells, especially at subcellular resolution. Although previous fluorescent Pt compounds have been reported elsewhere using fluorescein derivatives as the fluorophore, which are not ideal due to photobleaching and poor fluorescence *in vivo*.[21−23] Alternatively, BDP (4,4-difluoro-5,7-dimethyl-4-bora-3a,4a-diaza-s-indacene-3) derivatives have received considerable interest in bioimaging and intravital imaging because of their outstanding and desirable properties such as high absorption coefficients, sharp emissions, high fluorescence quantum yields, and excellent chemical and photostability.[24,25] However, relatively little attention has been paid to the use of BODIPY labeled Pt for studying their cellular uptake and distribution, although Miller et al. have reported Pt compounds conjugated with BDP.[26] In this work, we designed and synthesized fluorescent BODIPY-Pt conjugate (BODIPY-Pt), then studied its cellular uptake and cytotoxicities in human cervical carcinoma (HeLa) and human breast cancer (MCF-7) cell lines.

The 1,3,5,7-tetramethyl-8-(4-pyridyl)-4,4′-difluorobora-dia-zaindacene (BODIPY) was synthesized according to the literature,[27] and BODIPY-Pt was prepared by using the reported method (Scheme 1) in 48% yield,[1,28] but using

Scheme 1. Synthesis of BODIPY-Pt
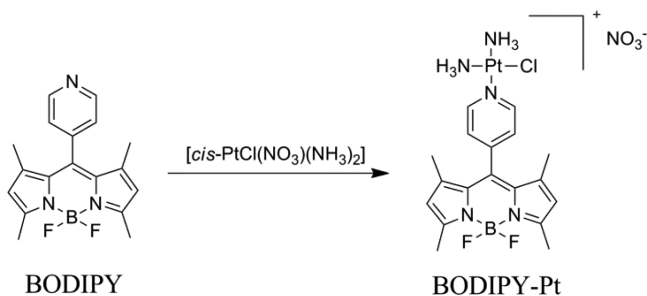
BODIPY as the imaging reporter. The structure of BODIPY-Pt was confirmed by proton nuclear magnetic resonance (^{1}H NMR) (Figure S1) and matrix-assisted laser desorption/ionization time-of-flight mass spectrometry (MALDI-TOF MS) (Figure S2). As shown in Figure S1, the signals for protons in pyridine ring in BODIPY are at 7.5 and 8.7 ppm, respectively, while the corresponding signals for BODIPY-Pt are observed at 7.7 and 8.9 ppm, which are down shifted due to the coordination of pyridyl groups to Pt. The peak at 590.2 in the MALDI-TOF MS spectrum is ascribed to the theoretical molecular weight of [BODIPY-Pt]$^+$. The ultraviolet visible (UV−vis) spectra of BODIPY and BODIPY-Pt in water are shown in Figure S3a, the absorption band of BODIPY is centered at 500 nm, while the absorption band of BODIPY-Pt is at 504 nm. As shown in Figure S3b, the maximum emission peaks are at 519 and 535 nm for BODIPY and BODIPY-Pt, respectively. It is also noteworthy that the incorporation of Pt makes the fluorescence quantum yield decrease from 0.23 to 0.04 by using rhodamine 6G as the reference, which is ascribed to the oxidative photoinduced electron transfer (PET) from the excited core of BODIPY to the pyridyl group.[29,30] Pt content of 26.7 wt % determined by inductively coupled plasma mass spectrometry (ICP-MS) was close to the theoretical content (30 wt %). These results indicated the desired product was obtained.

The biocompatibility of materials is very important for their biomedical applications. Herein, the biocompatibilty of BODIPY was evaluated by MTT (3-(4,5-dimethylthiazol-2-yl)-2,5-diphenyltetrazolium bromide) assays toward HeLa and MCF-7 cells. As shown in Figure S4, no obvious cytotoxicity was observed even at a concentration of 123 μM for BODIPY after 48 h.

In order to evaluate the biological activities of BODIPY-Pt and to identify the key targets, subcellular localization in HeLa cells was studied by using confocal laser scanning microscopy (CLSM). HeLa cells were incubated with BODIPY (5 μM) and BODIPY-Pt (5 μM) at 37 °C for 2 h, respectively. The cellular nuclei were selectively stained with 4′,6-diamidino-2-phenyl-indole (DAPI). Interestingly, neither BODIPY nor BODIPY-Pt was observed in the nuclei, and the fluorescence intensity of BODIPY-Pt was apparently higher than that of BODIPY (Figure 1a), although the fluorescence quantum yield of BODIPY-Pt (0.04) was lower than that of BODIPY (0.23). BODIPY-Pt exhibited significantly enhanced cellular uptake than BOIDPY. Then, flow cytometry was used to examine
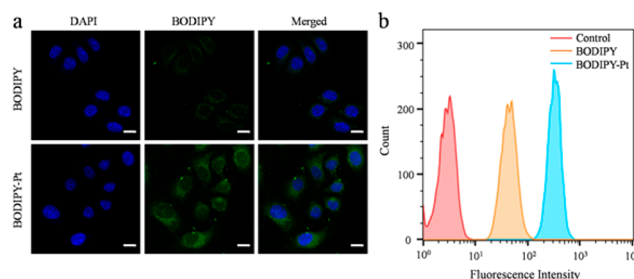
Figure 1. (a) CLSM images of HeLa cells incubated with BODIPY and BODIPY-Pt for 2 h at 37 °C at a concentration of 5 μM. All images show the nuclei (blue), BODIPY (green), and merged images. Scale bars represent 20 μm in all images. (b) Quantitative analysis by flow cytometry upon incubating HeLa cells with BODIPY or BODIPY-Pt (10 μM) at 37 °C for 1 h with cells untreated as a control.

quantitatively the cellular uptake of BODIPY-Pt. HeLa cells were incubated with 10 μM BODIPY or BODIPY-Pt at 37 °C for 1 h with cells untreated as a control. As shown in Figure 1b, almost all cells were able to internalize BODIPY and BODIPY-Pt since nearly 100% of cells indicated increased fluorescence except the control group. Compared to BODIPY, HeLa cells treated with BODIPY-Pt after 1 h showed maximum fluorescence intensity, which meant greater cellular uptake of BODIPY-Pt. This result is consistent with that of CLSM. The possible explanation for enhanced cellular uptake is that the positively charged Pt units facilitate the cellular uptake of the BODIPY-Pt conjugate,[31] because molecules with positive charges can enter into cells easier.

To obtain insight into the intracellular fate of BODIPY-Pt, colocalization experiments with a commercially available mitochondria-specific dye MitoTracker Red CM-H2XRos (MitoTracker Red) in HeLa cells were performed. HeLa cells were separately pretreated with BODIPY and BODIPY-Pt (5 μM each) for 2 h at 37 °C, respectively. The media were then replaced with MitoTracker Red (100 nM) and incubated for 30 min at 37 °C. The cellular nuclei were selectively stained with DAPI. In order to obtain a clear colocalization image, HeLa cells incubated with BODIPY were viewed under higher laser intensity relative to those incubated with BODIPY-Pt. As can be seen from Figure 2, both of them showed a distinct mitochondrial distribution, which was confirmed by monitoring
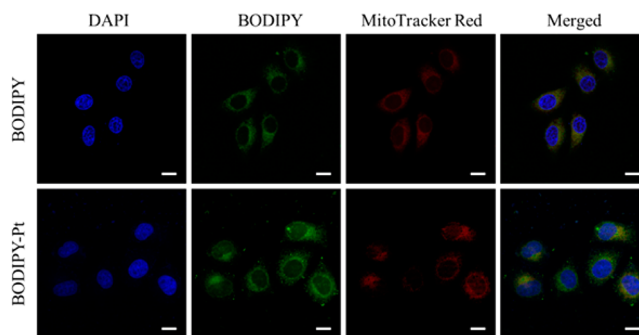
Figure 2. CLSM images of HeLa cells incubated with BODIPY and BODIPY-Pt for 2 h at 37 °C at a concentration of 5 μM. Cells are viewed in the blue channel for DAPI, the green channel for BODIPY, and the red channel for MitoTracker Red. The yellow areas in the merged pictures indicate colocalization of BODIPY or BODIPY-Pt within mitochondrial compartments. Scale bars represent 20 μm in all images.

colocalization with MitoTracker Red. These results indicated that BODIPY-Pt was localized predominantly in the mitochondria.

To examine whether the uptake of BODIPY-Pt was dependent on the mitochondrial membrane potential,[32] carbonyl cyanide *m*-chlorophenylhydrazone (CCCP) was used to treat the cells prior to the staining procedure. CCCP is an uncoupler that causes rapid acidification of the mitochondria and dysfunction of ATP synthase resulting in the decrease of the mitochondrial $\Delta\Psi_m$.[33] As shown in Figure 3a, when the cells were treated with 20 μM CCCP, weaker
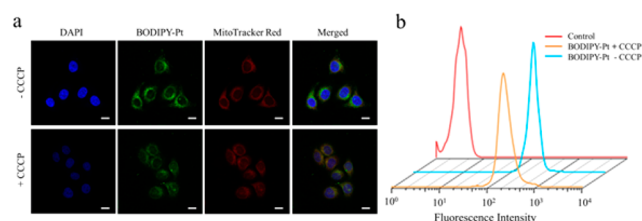
Figure 3. CLSM images (a) and flow cytometry (b) of HeLa cells pretreated with 20 μM CCCP for 45 min, and then incubated with BODIPY-Pt for 2 h at 37 °C at a concentration of 5 μM. Shown are the nuclei (blue), BODIPY-Pt (green), MitoTracker Red (red), and merged images. Scale bars represent 20 μm in all images.

mitochondria colocalization was observed, and the cellular uptake of BODIPY-Pt was reduced after CCCP treatment (Figure 3b). This result indicates BODIPY-Pt localizes in mitochondria and its cellular uptake is sensitive to the mitochondrial membrane potential.

We also quantified content of Pt in mtDNA from BODIPY-Pt and cisplatin. The HeLa cells were incubated with each of them at a concentration of 5 μM for 2 h. Then the collection and purification of the mtDNA was done by using a mitochondrial DNA isolation kit, and the Pt concentration in mtDNA was obtained by ICP-MS.[34,35] Agarose gel electrophoresis (Figure S5) demonstrated that the mtDNA (about 16.5 kb) had been isolated from the mitochondria of HeLa cells successfully. As shown in Figure S6, the Pt contents of BODIPY-Pt in the mtDNA are higher than that of cisplatin, which can also give a proof for the mitochondria localization of BODIPY-Pt.

Although the BODIPY-Pt could be internalized by HeLa cells and localized predominantly in the mitochondria, it was not clear whether there was still cytotoxicity of the fluorophore-labeled cisplatin. The cytotoxicity of BODIPY-Pt was investigated with free cisplatin as a positive control and blank culture medium without drugs as a negative control. Figure 4 shows the cell viabilities of HeLa (Figure 4a) and MCF-7
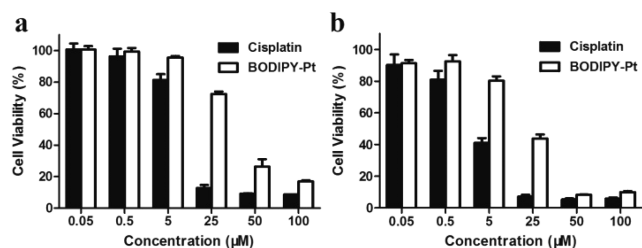
Figure 4. Viabilities of HeLa (a) and MCF-7 (b) cells treated with free cisplatin and BODIPY-Pt after incubation for 48 h at 37 °C. All the results were repeated three times and presented as mean ± SD.

(Figure 4b) cells after 48 h culture with different Pt formulations at various Pt concentrations. It can be seen that cytotoxicities of the tested formulations are all concentration dependent. The half maximal inhibitory concentration (IC$_{50}$) of cisplatin and BODIPY-Pt against HeLa and MCF-7 cell lines are summarized in Table 1. The inhibition efficacy of BODIPY-

Table 1. Cytotoxicities (IC$_{50}$ [μM]) of Cisplatin and BODIPY-Pt for HeLa and MCF-7 Cancer Cell Lines at 48 h

compd	HeLa	MCF-7
cisplatin	8.75 ± 0.24	3.43 ± 0.38
BODIPY-Pt	27.37 ± 1.14	12.14 ± 2.44

Pt is slightly lower than that of cisplatin, particularly at lower concentrations (5−25 μM). However, they exhibit similar efficacy compared with cisplatin at a higher concentration of 100 μM.

In summary, a BODIPY labeled Pt compound was successfully prepared via a convenient synthesis method. BODIPY-Pt was localized predominantly in the mitochondria and its cellular uptake is sensitive to the mitochondrial membrane potential. The Pt units facilitated the cellular uptake of the BODIPY-Pt conjugates. Although the cytotoxicity of BODIPY-Pt is mildly lower than that of cisplatin, we have made it possible to image Pt distribution in living cells. That is, BODIPY-Pt can fulfill the cytostatic and imaging functions simultaneously. Our proof of concept *in vitro* shows that BODIPY labeled Pt compounds represent an attractive approach to be optimized and developed in the future.

■ ASSOCIATED CONTENT

ⓢ Supporting Information

Details of chemical synthesis, structural analysis, and biological assays. This material is available free of charge via the Internet at http://pubs.acs.org.

■ AUTHOR INFORMATION

Corresponding Authors

*Tel: +86 431 85262775. E-mail: xiez@ciac.ac.cn.

*E-mail: zhengm@ciomp.ac.cn.

Notes

The authors declare no competing financial interest.

■ ABBREVIATIONS

BODIPY, (1,3,5,7-tetramethyl-8-(4-pyridyl)-4,4′-difluorobora diazaindacene); BODIPY-Pt, BODIPY-Pt conjugate; CLSM, confocal laser scanning microscopy; HeLa, human cervical carcinoma cells; MCF-7, human breast cancer cells; mtDNA, mitochondrial DNA; Dox, doxorubicin; NER, nucleotide excision repair; BDP, 4,4-difluoro-5,7-dimethyl-4-bora-3a,4a-diaza-s-indacene-3; ^{1}H NMR, proton nuclear magnetic resonance; MALDI-TOF MS, matrix-assisted laser desorption/ionization time-of-flight mass spectrometry; UV−vis, ultraviolet visible; MeOH, methanol; PET, photoinduced electron transfer; ICP-MS, inductively coupled plasma mass spectrometry; MTT, 3-(4,5-dimethylthiazol-2-yl)-2,5-diphenyl-tetrazolium bromide; DAPI, 4′,6-diamidino-2-phenylindole;

MitoTracker Red, MitoTracker Red CM-H2XRos; CCCP, carbonyl cyanide *m*-chlorophenylhydrazone; IC$_{50}$, half maximal inhibitory concentration

■ REFERENCES

(1) Naik, A.; Rubbiani, R.; Gasser, G.; Spingler, B. VisibleLight Induced Annihilation of Tumor Cells with Pt−Porphyrin Conjugates. *Angew. Chem., Int. Ed.* **2014**, *53*, 6938−6941.

(2) Jamieson, E. R.; Lippard, S. J. Structure, Recognition, and Processing of Cisplatin−DNA Adducts. *Chem. Rev.* **1999**, *99*, 2467−2498.

(3) Thayer, A. M. Pt drugs take their roll. *Chem. Eng. News* **2010**, *88*, 24−28.

(4) Lease, N.; Vasilevski, V.; Carreira, M.; de Almeida, A.; Sanau, M.; Hirva, P.; Casini, A.; Contel, M. Potential anticancer heterometallic Fe-Au and Fe-Pd agents: initial mechanistic insights. *J. Med. Chem.* **2013**, *56*, 5806−5818.

(5) Xiao, H.; Qi, R.; Liu, S.; Hu, X.; Duan, T.; Zheng, Y.; Huang, Y.; Jing, X. Biodegradable polymer − cisplatin(IV) conjugate as a pro-drug of cisplatin(II). *Biomaterials* **2011**, *32*, 7732−7739.

(6) Madias, N. E.; Harrington, J. T. Pt nephrotoxicity. *Am. J. Med.* **1978**, *65*, 307−314.

(7) Ekborn, A.; Laurell, G.; Andersson, A.; Wallin, I.; Eksborg, S.; Ehrsson, H. Cisplatin-induced hearing loss: influence of the mode of drug administration in the guinea pig. *Hear. Res.* **2000**, *140*, 38−44.

(8) Cheng, Q.; Shi, H.; Wang, H.; Min, Y.; Wang, J.; Liu, Y. The ligation of aspirin to cisplatin demonstrates significant synergistic effects on tumor cells. *Chem. Commun.* **2014**, *50*, 7427−7430.

(9) Pathak, R. K.; Marrache, S.; Choi, J. H.; Berding, T. B.; Dhar, S. The prodrug platin-A: simultaneous release of cisplatin and aspirin. *Angew. Chem.* **2014**, *53*, 1963−1967.

(10) Vik, R.; Busnelli, M.; Parolini, C.; Bjorndal, B.; Holm, S.; Bohov, P.; Halvorsen, B.; Brattelid, T.; Manzini, S.; Ganzetti, G. S.; Dellera, F.; Nygard, O. K.; Aukrust, P.; Sirtori, C. R.; Chiesa, G.; Berge, R. K. An Immunomodulating Fatty Acid Analogue Targeting Mitochondria Exerts Anti-Atherosclerotic Effect beyond Plasma Cholesterol-Lowering Activity in apoE$^{-/-}$ Mice. *PLoS One* **2013**, *8*, e81963.

(11) Lane, N. Mitochondrial disease: Powerhouse of disease. *Nature* **2006**, *440*, 600−602.

(12) Tranah, G. J.; Yokoyama, J. S.; Katzman, S. M.; Nalls, M. A.; Newman, A. B.; Harris, T. B.; Cesari, M.; Manini, T. M.; Schork, N. J.; Cummings, S. R.; Liu, Y.; Yaffe, K. Mitochondrial DNA sequence associations with dementia and amyloid-*β* in elderly African Americans. *Neurobiol. Aging* **2014**, *35*, 442.e1−442.e8.

(13) Ten, V. S.; Yao, J.; Ratner, V.; Sosunov, S.; Fraser, D. A.; Botto, M.; Sivasankar, B.; Morgan, B. P.; Silverstein, S.; Stark, R.; Polin, R.; Vannucci, S. J.; Pinsky, D.; Starkov, A. A. Complement Component C1q Mediates Mitochondria-Driven Oxidative Stress in Neonatal Hypoxic−Ischemic Brain Injury. *J. Neurosci.* **2010**, *30*, 2077−2087.

(14) Han, J.; Lee, T. H.; Tung, C.-H.; Lee, D. Y. Design and synthesis of a mitochondria-targeting carrier for small molecule drugs. *Org. Biomol. Chem.* **2014**, *12*, 9793−9796.

(15) Chamberlain, G. R.; Tulumello, D. V.; Kelley, S. O. Targeted Delivery of Doxorubicin to Mitochondria. *ACS Chem. Biol.* **2013**, *8*, 1389−1395.

(16) Marrache, S.; Pathak, R. K.; Dhar, S. Detouring of cisplatin to access mitochondrial genome for overcoming resistance. *Proc. Natl. Acad. Sci. U.S.A.* **2014**, *111*, 10444−10449.

(17) Galluzzi, L.; Senovilla, L.; Vitale, I.; Michels, J.; Martins, I.; Kepp, O.; Castedo, M.; Kroemer, G. Molecular mechanisms of cisplatin resistance. *Oncogene* **2012**, *31*, 1869−1883.

(18) Yu, Z. W.; Zhong, L. P.; Ji, T.; Zhang, P.; Chen, W. T.; Zhang, C. P. MicroRNAs contribute to the chemoresistance of cisplatin in tongue squamous cell carcinoma lines. *Oral Oncol.* **2010**, *46*, 317−322.

(19) Gagnon, V.; Mathieu, I.; Sexton, E.; Leblanc, K.; Asselin, E. AKT involvement in cisplatin chemoresistance of human uterine cancer cells. *Gynecol. Oncol.* **2004**, *94*, 785−795.

(20) Yang, Z.; Schumaker, L. M.; Egorin, M. J.; Zuhowski, E. G.; Guo, Z.; Cullen, K. J. Cisplatin preferentially binds mitochondrial DNA and voltage-dependent anion channel protein in the mitochondrial membrane of head and neck squamous cell carcinoma: possible role in apoptosis. *Clini. Cancer Res.* **2006**, *12*, 5817−5825.

(21) Kalayda, G. V.; Zhang, G.; Abraham, T.; Tanke, H. J.; Reedijk, J. Application of Fluorescence Microscopy for Investigation of Cellular Distribution of Dinuclear Pt Anticancer Drugs. *J. Med. Chem.* **2005**, *48*, 5191−5202.

(22) Liang, X. J.; Finkel, T.; Shen, D. W.; Yin, J. J.; Aszalos, A.; Gottesman, M. M. SIRT1 contributes in part to cisplatin resistance in cancer cells by altering mitochondrial metabolism. *Mol. Cancer Res.* **2008**, *6*, 1499−1506.

(23) Katano, K.; Safaei, R.; Samimi, G.; Holzer, A.; Tomioka, M.; Goodman, M.; Howell, S. B. Confocal Microscopic Analysis of the Interaction between Cisplatin and the Copper Transporter ATP7B in Human Ovarian Carcinoma Cells. *Clin. Cancer Res.* **2004**, *10*, 4578−4588.

(24) Li, Z.; Zheng, M.; Guan, X.; Xie, Z.; Huang, Y.; Jing, X. Unadulterated BODIPY-dimer nanoparticles with high stability and good biocompatibility for cellular imaging. *Nanoscale* **2014**, *6*, 5662−5665.

(25) Quan, L.; Liu, S.; Sun, T.; Guan, X.; Lin, W.; Xie, Z.; Huang, Y.; Wang, Y.; Jing, X. Near-infrared emitting fluorescent BODIPY nanovesicles for in vivo molecular imaging and drug delivery. *ACS Appl. Mater. Interfaces* **2014**, *6*, 16166−16173.

(26) Miller, M. A.; Askevold, B.; Yang, K. S.; Kohler, R. H.; Weissleder, R. Pt Compounds for High-Resolution In Vivo Cancer Imaging. *ChemMedChem* **2014**, *9*, 1131−1135.

(27) Bartelmess, J.; Weare, W. W.; Latortue, N.; Duong, C.; Jones, D. S. meso-Pyridyl BODIPYs with tunable chemical, optical and electrochemical properties. *New J. Chem.* **2013**, *37*, 2663−2668.

(28) Park, G. Y.; Wilson, J. J.; Song, Y.; Lippard, S. J. Phenanthriplatin, a monofunctional DNA-binding Pt anticancer drug candidate with unusual potency and cellular activity profile. *Proc. Natl. Acad. Sci. U.S.A.* **2012**, *109*, 11987−11992.

(29) Ulrich, G.; Ziessel, R. Convenient and Efficient Synthesis of Functionalized Oligopyridine Ligands Bearing Accessory Pyrromethene-BF2 Fluorophores. *J. Org. Chem.* **2004**, *69*, 2070−2083.

(30) Olmsted, J. Calorimetric determinations of absolute fluorescence quantum yields. *J. Phys. Chem.* **1979**, *83*, 2581−2584.

(31) Zhu, Z.; Wang, X.; Li, T.; Aime, S.; Sadler, P. J.; Guo, Z. Pt(II)-Gadolinium(III) Complexes as Potential Single-Molecular Theranostic Agents for Cancer Treatment. *Angew. Chem.* **2014**, *53*, 13225−13228.

(32) Yuan, H.; Cho, H.; Chen, H. H.; Panagia, M.; Sosnovik, D. E.; Josephson, L. Fluorescent and radiolabeled triphenylphosphonium probes for imaging mitochondria. *Chem. Commun.* **2013**, *49*, 10361−10363.

(33) Leung, C. W.; Hong, Y.; Chen, S.; Zhao, E.; Lam, J. W.; Tang, B. Z. A photostable AIE luminogen for specific mitochondrial imaging and tracking. *J. Am. Chem. Soc.* **2013**, *135*, 62−65.

(34) Li, J.; Hu, X.; Liu, M.; Hou, J.; Xie, Z.; Huang, Y.; Jing, X. Complex of cisplatin with biocompatible poly(ethylene glycol) with pendant carboxyl groups for the effective treatment of liver cancer. *J. Appl. Polym. Sci.* **2014**, *131*, 40764.

(35) Xiao, H.; Song, H.; Yang, Q.; Cai, H.; Qi, R.; Yan, L.; Liu, S.; Zheng, Y.; Huang, Y.; Liu, T.; Jing, X. A prodrug strategy to deliver cisplatin(IV) and paclitaxel in nanomicelles to improve efficacy and tolerance. *Biomaterials* **2012**, *33*, 6507−6519.